Journal of Surgical Research ■, 1–10 (2010)
doi:10.1016/j.jss.2009.11.723

Silencing Id-1 with RNA Interference Inhibits Adenoid Cystic Carcinoma in Mice

Zhenggang Chen, M.D.,* Shaohua Liu, Ph.D., M.D.,† Tomoki Sumida, D.D.S., Ph.D.,‡ Shanzhen Sun, Ph.D., M.D.,§ Yuan Wei, Ph.D., M.D.,|| Meng Liu, Ph.D., M.D.,¶ Zuoqing Dong, M.D.,† Fan Zhang, M.D.,# Hiroyuki Hamakawa, D.D.S., Ph.D.,‡ and Fengcai Wei, Ph.D., M.D.†,[1]

*School of Stomatology, Shandong University, Jinan, People's Republic of China; †Department of Oral and Maxillofacial Surgery, Qilu Hospital, Shandong University, Jinan, People's Republic of China; ‡Department of Oral and Maxillofacial Surgery, Ehime University School of Medicine, Ehime, Japan; §Department of Pathology, School of Stomatology, Shandong University, Jinan, People's Republic of China; ||Department of Geriatric Medicine, Qilu Hospital, Shandong University, Jinan, People's Republic of China; ¶Department of Neurosurgery, Qilu Hospital, Shandong University, Jinan, People's Republic of China; and #Department of Orthodontics, School of Stomatology, Shandong University, Jinan, People's Republic of China

Submitted for publication July 13, 2009

Background. **The helix-loop-helix (HLH) protein Id-1 (inhibitor of DNA binding/differentiation) has been demonstrated to play an important role in tumor development. Our previous *in vitro* research has shown that Id-1 is a potential target in the treatment of human adenoid cystic carcinoma (ACCM). The purpose of this study was to analyze the influence of Id inhibition on ACCM in mice.**

Materials and Methods. **To suppress the expression of Id-1 gene, we used lentivirus-mediated RNA interference to silence the Id-1 gene post-transcriptionally in ACCM models that stably express GFP in mice. Tumor development was evaluated by size measurement. Effects of Id-1 siRNA on mRNA and protein expression of Id-1 were analyzed using quantitative reverse transcriptase polymerase chain reaction (RT-PCR) and Western blotting respectively. Ki-67 expression was measured by immunohistochemistry. *In vitro* studies of Hoechst staining for cell apoptosis, Boyden-chamber assay for cell invasion, and MTT-tests for cell growth were performed as well.**

Results. **Id-1 knockdown resulted in inhibition of tumor growth in mice. Id-1 siRNA significantly decreased not only Id-1 in mRNA and protein level, but also Ki-67 expression. In addition, apoptosis was induced and cell proliferation activity and invasion were significantly reduced.**

Conclusions. **Lentivirus-mediated gene knockdown by silencing Id-1 constitute a valid methodological approach, which may represent an attractive, potent and specific therapeutic tool for the treatment of ACCM.**

Key Words: **adenoid cystic carcinoma; RNA interference; lentivirus; gene therapy; Id-1 gene.**

INTRODUCTION

Adenoid cystic carcinoma (ACC) is a unique slow-growing but highly malignant tumor of the salivary gland with noticeable capacities for diffuse invasion and high frequency of distant metastasis [1, 2]. The mortality rate of these patients, owing to late recurrences or metastases, even for low-grade tumors, is particularly high, with reported data of over 50% survival at 5 y and less than 20% survival at 10–20 years [3]. Approximately 40% to 60% of patients develop distant metastases, despite slow growth and good local control of the tumor [3]. Surgery, usually followed by postoperative radiotherapy, is the principal and standard primary treatment due to the resistance of ACCs to chemotherapy and radiotherapy; however, there is uncertainty about the systemic management of ACCs. Adenoid cystic carcinoma-M (ACCM) screened out of ACC-2 is characterized by rapid growth and is very susceptible for genetic experimentation [4, 5].

Id-1 (inhibitor of differentiation/DNA binding), one member of the helix-loop-helix (HLH) transcription factors that is an important regulator of cellular

[1] To whom correspondence and reprint requests should be addressed at Department of Oral and Maxillofacial Surgery, Qilu Hospital, Shandong University, No.107 West Wenhua Road, Jinan 250012, People's Republic of China. E-mail: weifengcai2009@163.com.

0022-4804/09 $36.00

differentiation and proliferation lacks a basic domain for DNA binding. Therefore, it acts as a dominant negative HLH protein by forming high-affinity heterodimers with other bHLH proteins, thereby preventing them from binding to DNA and inhibiting transcription of differentiation-associated genes [6]. It has been shown to be up-regulated in many types of human cancers [6, 7] such as gastric carcinoma [8], breast cancer [9], prostate carcinoma [10], and ovarian cancer [11]. Its expression level is directly associated with poor clinical outcomes and drug resistance [12]. Previous findings have verified the high expression of Id-1 in ACC tumors [13, 14], which is consistent with this view. In all Id-proteins (Id-1, Id-2, Id-3, and Id-4), Id-1 plays the most crucial role in head and cervical cancer [15, 16]. Because of close correlation with several other important oncogenes [17, 18] and non-expression in most mature adult tissues [17], therapeutic strategies based on targeting Id-1 expression might be effective in ACCM tumors with a high expression of Id-1.

Inhibiting the expression of a specific gene can be achieved by post-transcriptional gene knockdown through RNA interference (RNAi), which has emerged as a powerful tool to induce loss-of-function phenotypes by post-transcriptional silencing of gene expression [19]. Some research support that RNAi can be successfully applied to inhibit tumor development [20–23]. For therapeutic purposes, it is essential to introduce dsRNA inside the cells, so that they can recognize the target genes and cause their suppression, thereby preventing the disease. Virus-based therapy, especially lentivirus-based therapy, has shown promising results in the treatment of both inherited and acquired diseases [24].

In our ACCM-GFP mouse model, we show that the local delivery of Id-1-siRNA sufficiently suppressed the Id-1 gene, as detected by RFP. Silencing of Id-1 decreased the gene expression at both mRNA and protein levels. Id-1 silencing resulted in inhibited ACCM tumor growth, reduced tumor cell proliferation and invasion, and induced apoptosis. These data suggest that the silencing of Id-1 with lentivirus-mediated RNAi is an attractive strategy for the treatment of ACCM.

MATERIALS AND METHODS

Isolation and Culture of ACCM-GFP Cells

The pLEGFP-N1 plasmids (kindly presented by Stomatology School, Shandong University) were transfected into DH5α cells and identified by restriction endonuclease analysis. Viral supernatant containing EGFP virus was produced by packaging cell line PT67 (Shanghai Institutes for Biological Sciences, SIBS [25]. Briefly, 2×10^5 PT67 cells were plated into a 6-well dish 12 to 24 h before transfection at 80% confluence; 25 μL DOTAP (Roche, Germany) was added, then PT67 cells were transfected and screened with 800 μg/mL G418. After collecting viral supernatant through a 0.45 μm cellulose acetate filter, viral titer was determined by NIH3T3 cells (SIBS) [26]. 1×10^5 ACCM cells (derived from human salivary gland adenoid cystic carcinoma, China Center for Type Culture Collection, CCTCC) in a 6-well plate were exposed to viral supernatant at a multiplicity of infection, in the presence of 8 μg/mL polybrene for 24 h. Subsequently, the viral supernatant was replaced with fresh medium. ACCM-GFP cells were acquired with 300 μg/mL G418 selection for 2 wk and then were collected and counted, split one cell per well in a 96-well plate. Colonies were grown in DMEM (Invitrogen, Carlsbad, CA, USA) supplemented with 10% fetal bovine serum (FBS) and antibiotics (100 U/mL penicillin, 100 U/mL streptomycin) at 37 °C, 5%CO_2.

Cell Numbers Calculation

ACCM-GFP cells, 1×10^4, were plated in a 6-well dish with DMEM containing 10% FBS. For evaluation of cell growth, the number of viable cells cultured in the plate was counted everyday with Neubauer's counting method after suspension.

Tumor Model and RNAi

ACCM-GFP cells, 2×10^5, in 0.1 mL medium were harvested and injected submucosally into lingual central part at the cross-point of forward one-third and backward two-third in 60 BALB/c nu/nu male mice (SLAC, Shanghai, China). They were 6 wk old, with a body weight of 20–25 g. Three weeks later, 10^8 TU Id-1-siRNA-lentivirus and NC-siRNA-lentivirus (pGCSIL-RFP, Id-1-siRNA sequence: CATGAACGGCTGTTACTCA, NC-siRNA sequence: TTCTCCG AACGTGTCACGT, Shanghai GeneChem, China) were injected into 48 and 6 tumors, respectively, and each was in 20 μL DMEM containing 10% FBS and 5 μg/mL polybrene. Mice were treated in accordance with the guidelines provided by Shandong University, China.

Transduction Efficiency Assay

Infection of ACCM cells by Id-1-siRNA-lentivirus in vitro was applied to analyze the transduction efficiency. ACCM cells, 10^4, were seeded in each well of a 24-well plate. The cells were infected in DMEM containing 10% FBS and 5 μg/mL polybrene when the confluence was about 30%–40% and Id-1-siRNA-lentivirus was introduced at a multiplicity of infection (MOI) of 50 for 24 h. At different time points, cells were harvested and resuspended in PBS with the final concentration of 5×10^5/mL. For FACS analysis, 5×10^3 cells were counted in a cytofluorimeter (FACS Calibur, BD, Franklin Lakes, NJ, USA).

Tumor Size Measurement and Fluorescence Photography

Each tumor was measured every 2 d by using a caliper and the following formula was used to calculate tumor volumes $= 1/2 \times A \times B^2$, where A and B represent the larger and smaller tumor diameters, respectively [7]. Graphs were plotted to illustrate tumor growth in each group. Mice were photographed for fluorescent images by KODAK Image Station (IS2000 MM; Eastman Kodak Rochester, NY). The mice were scanned with fluorescence with excitation maximum 465 and 560 nm for GFP and RFP, respectively.

Quantitative Reverse Transcription Polymerase Chain Reaction (RT-PCR) Analysis

Mice were sacrificed at d 3, 4, 5, 6, 7, 10, and 14 after RNAi. After isolation of total RNA by Trizol Reagent (Gibco, Grand Island, NY, USA), RNA concentration and quality were assessed spectrophotometrically at wavelengths 260 and 280 nm. Equal amount of RNA (500 ng) from different tumors was reverse transcribed as templates in 20 μL of reverse transcriptase (RT) reaction. PCR mixture contained: 10 mM Tris-HCl (pH8.0), 50 mM KCl, 2.5 mM $MgCl_2$, 0.3 mM dNTP each, 0.3 μM forward and reverse primers, 0.2 μM TaqMan probe, 1.5 U

Taq DNA Polymerase (Promega, Madison, Wl) and 2 μL cDNA. β-Actin was detected as an internal control. The sequences of primers and TaqMan probes are, for Id-1, forward: 5'-TCTACGACATGAACGGCTG-3'; reverse: 5'-GGTCCCTGAT
GTAGTCGAT-3'; probe: 5'-CTCAAGGAGCTGGTGCCTACC-3'; for β-actin, forward: 5'-GCCAACACAGTGCTGTCT-3'; reverse: 5'-AGGA GCAATGATCTTGATCTT-3'; probe: 5'-ATCTCCTTCTGCATCCT GT-3'. PCR was performed on FTC-2000 fluorescent quantitative PCR detection system (Funglyn Biotech, Toronto, Canada) with the following parameters: initial denaturation at 94 °C for 1 min followed by 45 cycles of 94 °C 20 s, 52 °C 20 s, and 72 °C 30 s, and then a final extension at 60 °C for 5 min. The amplification curves were analyzed and Ct values were determined. Folds of increase were used to quantify Id-1 mRNA expression, with the average $2^{-\Delta\Delta Ct}$ values of ACCM-GFP tumor tissues taken as 1 [27].

Western Blot Analysis

Proteins were extracted from tumors and quantified with nuclear and cytoplasmic Protein Extraction Kit and BCA Protein Assay Kit (Beyotime Institute of Biotechnology, Jiangsu, China), respectively. Samples (30 μg) were separated on 5% stacking, 10% separating SDS-polyacrylamide gels, and subsequently transferred onto PVDF Membrane (Nippon Genetics, Tokyo, Japan) at 90 V for 35 min. The membrane was blocked, washed, and incubated with the primary antibody (purified rabbit polyclonal, Santa Cruz Biotechnology, Inc., Santa Cruz, CA) for anti-Id-1 (diluted 1/100 with TBST) and anti-β-actin (diluted 1/1000 with TBST), respectively, with overnight shaking. The primary antibody was probed with a peroxidase-conjugated AffiniPure Goat Anti-Rabbit IgG (Zhongshan Goldenbridge Biotechnology, Beijing, China, diluted 1/1000). After washing with TBST, the membrane was applied with Diaminobenzidine DAB kit (USCN Life Science Inc., Wuhan, China), developed, and photos were taken with KODAK Image Station (IS2000 MM; Eastman Kodak Rochester, NY). The expression of Id-1 protein was standardized to the internal standard, β-actin.

Immunohistochemistry Analysis

Tumor sections (5 μm) were de-paraffinized, rehydrated by serial ethanol dilutions, washed with Tris-buffered saline, and processed using a streptavidin-biotin-peroxidase complex method. Endogenous peroxidase activity was blocked for 30 min with a buffer solution containing peroxide, followed by antigen retrieval (citrate buffer, pH 6.0, 20 min). Incubation with the primary antibody (anti-Ki67; Immunotech, Beckman Coulter, Fullerton, CA; dilution 1:100, 60 min, RT) was followed by the secondary antibody (biotinylated horse anti-mouse, diluted 1:500, Vector BA-2000; Vector Laboratories, Burlingame, CA), followed by streptavidin-biotin complex, diluted 1:1000 (Immunotech). Slides were counterstained with hematoxylin before dehydrating and mounting. The fraction of Ki-67-positive cells was determined by counting 100 cells in six random fields from each section.

Cell Apoptosis Analysis

Apoptosis was measured using Hoechst 33258 staining (Apoptosis-Hoechst staining kit, Beyotime Biotechnology, Jiangsu, China). Briefly, cells were first immersed in 0.5 mL of methanol for 15 min and then rinsed with PBS twice; 1 μg/mL Hoechst 33258 reagent was used to stain the apoptotic cells in dark at RT for 10 min, after which the cells were again washed with PBS twice. The stained cells were examined and immediately photographed under a fluorescence microscope (Olympus IX81; Shinjuku-ku, Tokyo, Japan) with excitation wavelength of 330–380 nm. Apoptotic cells were identified on the basis of morphologic changes in their nuclear assembly, e.g., chromatin condensation and fragmentation. In each group, six microscopic fields were selected randomly and apoptotic cell death was quantified as percent apoptotic cells per total blue fluorescent protein-positive cells. In order to avoid the interference arising from GFP, we used ACCM cells in stead of ACCM-GFP cells.

Matrigel Invasion Assay

Cell invasion was assayed using a Boyden chamber cell with culture-chamber-insert system (BD Bioscience, Franklin Lakes, NJ, USA) with an 8 μm polyethylene terephthalate (PET) membrane. The upper chamber of transwell was coated with 50 μg Matrigel (BD Bioscience) for 1 h at 37 °C and then placed into 24-well chambers. Five days after RNAi, cells infected with lentivirus vectors and ACCM-GFP cells were seeded into the upper chamber (2×10^4 cells in 200 μL serum-free DMEM), and incubated for 24 h at 37 °C. The non-migrating cells were removed from the upper side of the filters with cotton swab. Cells on the lower side of the membrane were fixed, stained with Wright's stain, counted in six random high-power fields, and photographed.

Methyl Thiazolyl Tetrazolium (MTT) Assay

Cells at a concentration of 10^3 per well were seeded in the 96-well plate and incubated for 24 h and then infected with lentivirus particles (the same method for Id-1-siRNA-lentivirus as NC-siRNA-lentivirus was mentioned in part of transduction efficiency assay). For this assay, the cells were incubated with 0.5 mg/mL MTT (Sigma-Aldrich, St. Louis, MO, USA). Four hours later, the medium was replaced with 100 μL dimethyl sulfoxide (DMSO) (Sigma-Aldrich) and vortexed for 10 min. Absorbance was then recorded at 490 nm using an enzymatic labeling instrument. Cell viability (%) was calculated as percent of control cells (ACCM). Each experiment was performed four times independently. In order to avoid the interference arising from GFP, we used ACCM cells in stead of ACCM-GFP cells.

Statistical Analysis

Data are presented as means ± SD from at least three experiments. The statistical analyses were performed with SPSS 12.0 (SPSS Inc., Chicago, IL). A P value < 0.05 was considered as statistically significant. Differences were determined with one-way analysis of variance and Tukey *post-hoc* test for multiple comparisons.

RESULTS

Similarity Between the Character of ACCM and ACCM-GFP Cells

In order to study the difference between ACCM and ACCM-GFP cells, we did morphologic observation and analyzed cell proliferation, cell invasion, and Western blot. ACCM-GFP cells showed no significant difference from ACCM cells in morphology, Id-1 protein expression, cell proliferation, and invasion ability (Fig. 1). These data indicated that our studies on ACCM-GFP cells can be established as equivalent to the research on ACCM cells.

Establishment of tumor model and high transduction efficiency

Fluorescent xenograft models with a long-term stable expression of GFP had been created successfully (Fig. 2A). Even a micro lymphatic metastasis could be detected in this model without any clinical palpable nodes. Meanwhile, transduction efficiency *in vitro* was evaluated by flow cytometry (Fig. 2B). With the stable

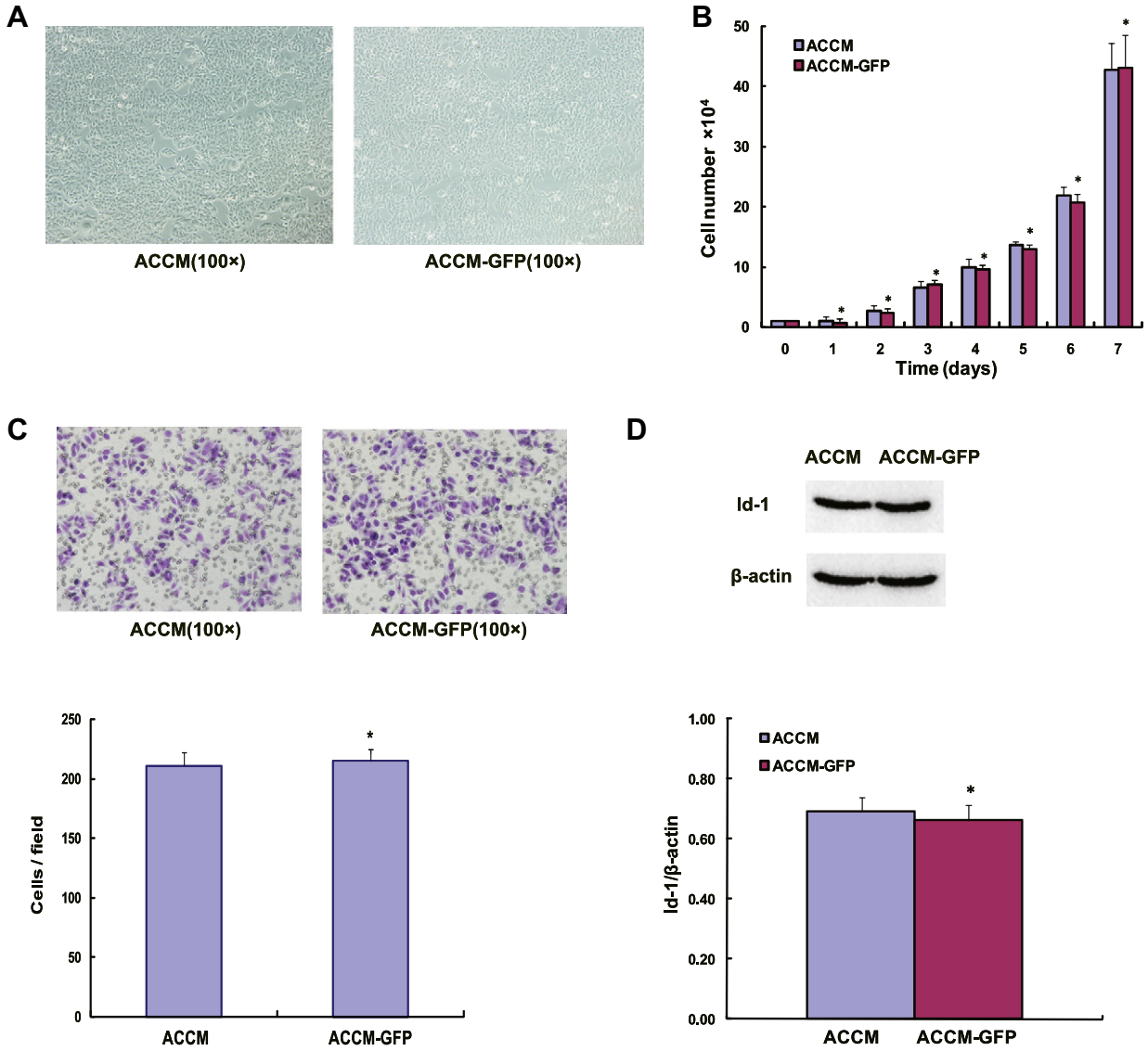

FIG. 1. Similarity between ACCM-GFP and ACCM cells. (A) ACCM-GFP cells show similar morphologic characters to ACCM cells. (B) ACCM-GFP cells and ACCM cells proliferate at the similar speed ($^*P > 0.05$). (C) No significant difference of invasiveness between ACCM-GFP cells and ACCM cells is shown ($^*P > 0.05$). (D) Western blot analysis for the extracted Id-1 protein from six independent experiments indicates that ACCM-GFP cells have the similar Id-1 protein expression to ACCM cells ($^*P > 0.05$). A representative image is provided.

expression of RFP, the high transduction efficiency of 83.5%, 68.45%, and 24.89% could be detected 72, 48, and 24 h after lentiviral infection, respectively. It was clear that this model was ideal for the next consecutive studies.

Analysis of Tumor Size Measurement, quantitative RT-PCR, Western Blot and Immunohistochemistry

Generally, 3–4 days after inoculation, mice developed palpable tumors. As shown in Fig. 3A, only 12 d after the infection with RNAi-containing lentivirus particles, tumor growth began to decrease. The tumor volumes in original ACCM-GFP and NC-siRNA-lentivirus group were $523.12 \pm 20.30\ mm^3$ and $558.21 \pm 50.95\ mm^3$ respectively, whereas the final tumor volume was $318.22 \pm 40.59\ mm^3$ in Id-1-siRNA-lentivirus group (on the 16^{th} day after RNAi treatment, $n = 6$ per group, $^*P < 0.01$).

To study the role of RNAi on the regulation of Id-1 expression and to determine its potential as a therapeutic target, we examined the mRNA expression of Id-1 by quantitative RT-PCR. Until the third day after injection, Id-1-siRNA-lentivirus-treated tumors, NC-siRNA-lentivirus-treated tumors, and ACCM-GFP tumors showed no reduction in the levels of Id-1,

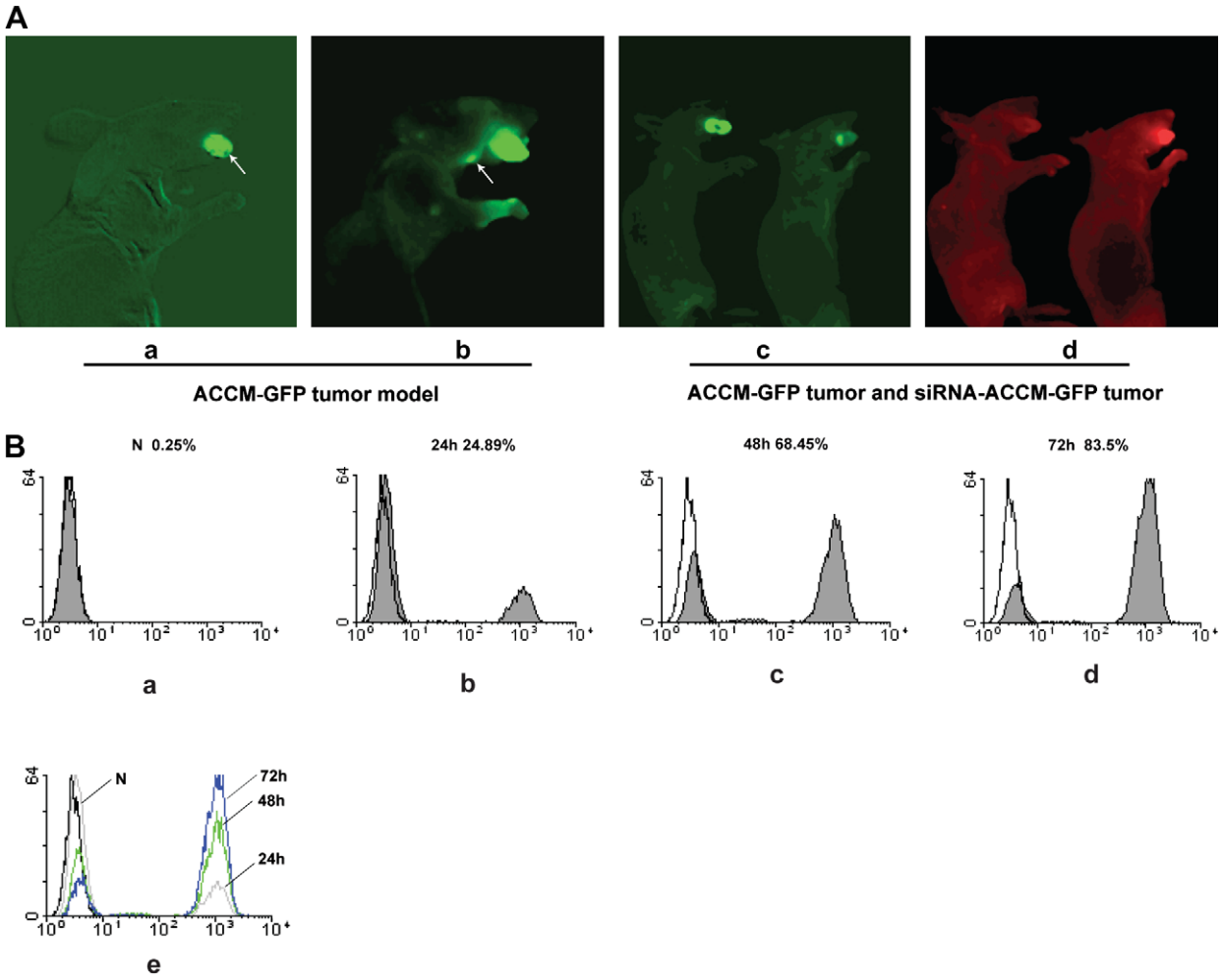

FIG. 2. Established ACCM-GFP animal model and FACS analysis of transduction efficiency. (A) Three weeks after ACCM-GFP cells orthotopic injection, the tumor will stably emit strong green fluorescence. We can find compartments inside the tumor and irregular tumor border, which is consistent with the biological behavior of ACCM tumors (arrow in a) and the lymphatic node involved by ACCM-GFP cells (arrow in b). Pictures (c) and (d) show fluorescent images of ACCM-GFP tumor (left mouse) and Id-1-siRNA-lentivirus-treated ACCM-GFP tumor (right mouse) scanned with 465 and 560 nm for detection of GFP and RFP, respectively. Infected and uninfected tumors can be observed easily, and it shows the high transduction efficiency by multiple intratumoral injections as well. (B) Illustrates that lentivirus has a potent ability to infect and the efficiency reaches a high level of 83.5% 72 h after infection (e). N stands for uninfected cells as a blank group in the assessment (a).

whereas those infected with Id-1-siRNA-lentivirus for more than 3 d showed significantly reduced levels of mRNA (Fig. 3B, $^*P < 0.01$). β-Actin quantitative RT-PCR was provided as loading controls.

To examine the effect of RNAi on Id-1 protein, tumors were analyzed by immunoblotting (Fig. 3C). The expression was markedly down-regulated in tumors from the fourth day of infection with Id-1-siRNA-lentivirus ($^*P < 0.01$), while it remained similar in blank control, NC-siRNA, and Id-1-siRNA group infected for no more than 3 d. These data indicated that both expression of Id-1 mRNA and protein dropped significantly from the fourth day of RNAi.

Immunohistochemical staining showed 78.67% ± 2.42% Ki-67 positive cells in tumors treated with NC-siRNA-lentivirus and 82.17% ± 3.54% in ACCM-GFP tumors (Fig. 3D, $P > 0.05$) on the seventh day after RNAi. On the other hand, cellular proliferation indices of tumors derived from Id-1-siRNA-lentivirus-treated mice, with a positive rate of 55.5% ± 4.14%, differed significantly from others ($^*P < 0.01$), indicating that blocking Id-1 expression did reduce the rate of cell replication.

Analysis of Cell Apoptosis, Invasion and MTT *In Vitro*

We showed that cells in culture after 5 d of infection with Id-1-siRNA exhibited lots of apoptosis, which was characterized by pyknotic and fragmented nuclei (Fig. 4A). Condensed bright apoptotic nuclei were readily observed amidst the transducted cells. In control

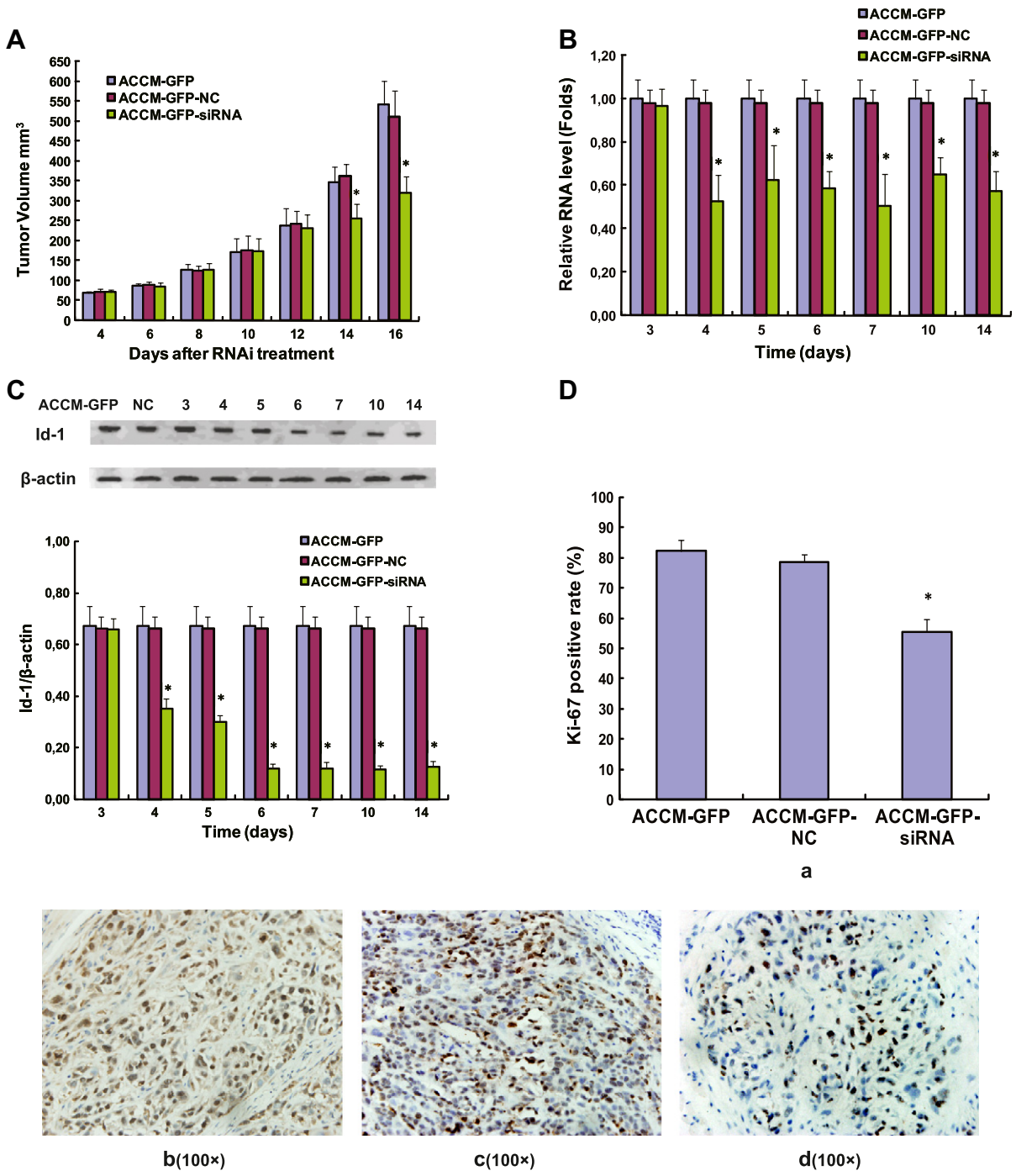

FIG. 3. RNAi inhibits the expression of Id-1 and Ki-67 *in vivo*. (A) Significant size reduction of ACCM-GFP tumors can be detected 12 d after intratumoral injection of Id-1-siRNA-lentivirus ($n = 6$ per group, $^*P < 0.01$). (B) Quantitative RT-PCR analysis for Id-1 in ACCM-GFP tumors, ACCM-GFP tumors treated with NC-siRNA-lentivirus and Id-1-siRNA-lentivirus respectively ($n = 6$ per group, $^*P < 0.01$). (C) Western blot analysis for Id-1 protein level shows the conspicuous decreasing tendency with the time ($^*P < 0.01$). (D) Tumor cells proliferation was quantified by Ki-67 immunohistochemistry, displaying large fraction of Ki-67-positive cells in ACCM-GFP tumors (b) and NC-Lentivirus-treated ACCM-GFP tumors (c), and fewer in siRNA-lentivirus-treated ACCM-GFP tumors (d) (7 d after RNAi, $^*P < 0.01$).

cultures, round and large nuclei appeared with regular contours, and cells with smaller nuclei and condensed chromatin were rarely seen.

Repression of Id-1 expression in ACCM-GFP was found to inhibit invasion *in vitro* (Fig. 4B). The mean invasion index of cells infected with Id-1-siRNA-lentivirus was 137.33 ± 6.74, whereas the means were 215 ± 9.38 and 205.67 ± 5.54 in ACCM-GFP group and NC-siRNA-lentivirus-treated group, respectively ($^*P < 0.01$).

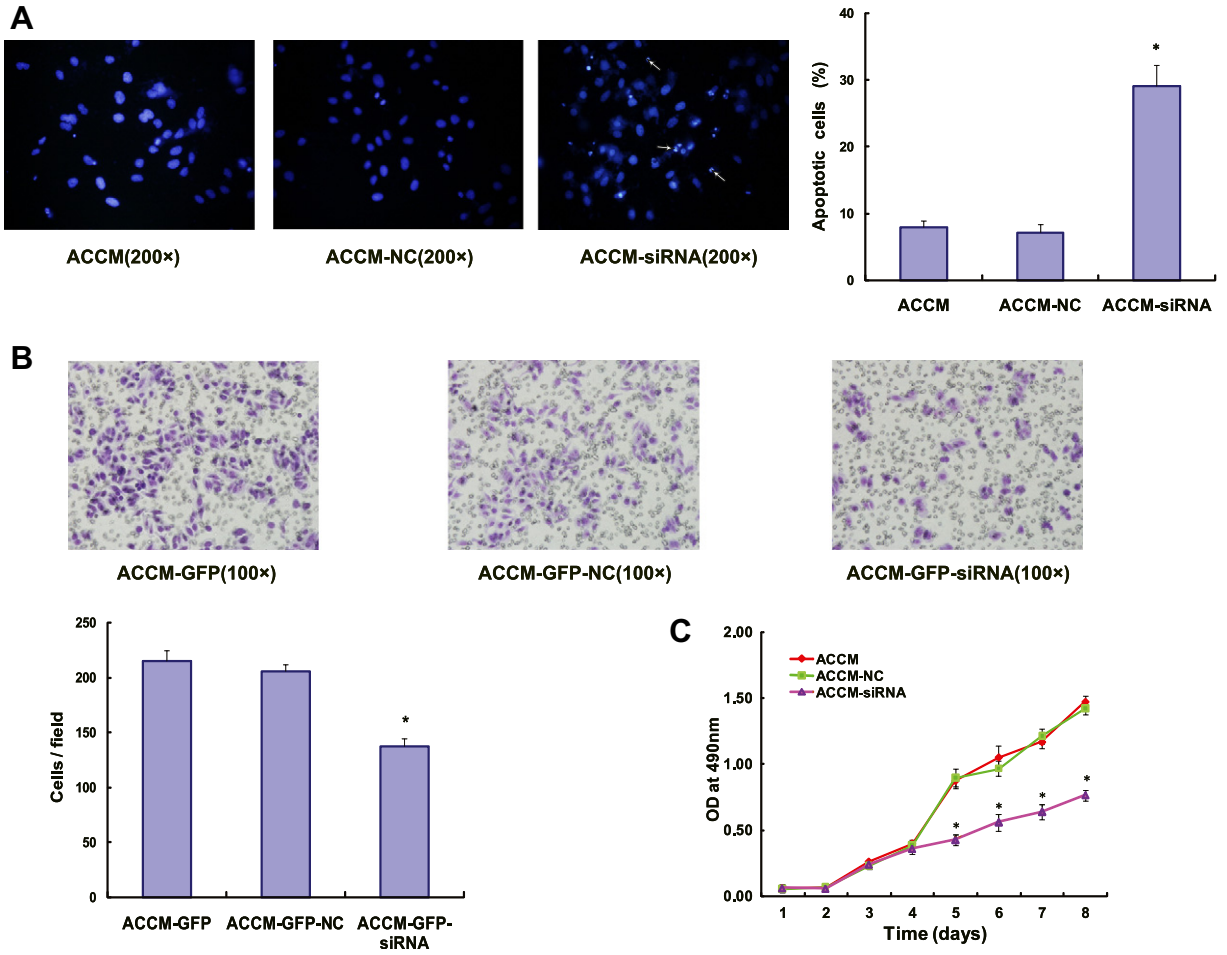

FIG. 4. RNAi induces cell apoptosis, inhibits cell invasion and arrests cell proliferation *in vitro*. (A) Morphologic changes in the nuclei of ACCM cells (arrows) induced by Id-1-siRNA-lentivirus and selected fields illustrating occurrence of apoptosis are shown. Cells with condensed chromatin are defined as apoptotic cells. Cell apoptosis increased dramatically (*$P < 0.01$). (B) Cell invasiveness was examined with Matrigel-coated invasion chambers and RNAi inhibits invasion of ACCM-GFP cells (5 d after RNAi, *$P < 0.01$). (C) RNAi reduces cell viability which was assayed by MTT (*$P < 0.01$).

MTT assays (Fig. 4C) showed that Id-1-siRNA-lentivirus-treated tumor cells grew significantly more slowly than others (*$P < 0.01$). No significant difference was detected in cells treated with NC-siRNA-lentivirus compared with untreated cells.

DISCUSSION

In an attempt to investigate the effect of gene silencing of RNAi on ACCM tumors, we established a type of fluorescent tumor model *in vivo*. Compared with other ACCM xenograft models [20], this one enabled direct visualization of tumor growth and invasion within viable tissues. Furthermore, orthotopic implantation is of particular importance with regard to the accurate preclinical evaluation of new antimetastatic agents [28]. The lymphatic node involved is shown clearly, indicating that metastases could be detected in an early stage. As we know, a nude mouse is a mouse from a strain with a genetic mutation that causes a deteriorated or absent thymus, resulting in an inhibited immune system due to a greatly reduced number of T cells. It is valuable to research because it can receive many different types of tissue and tumor grafts. ACCM that grows slowly in clinic can develop rapidly in nude mice even in 3 wk in our research. Without limitation of surrounding organ to tumor development, the tumors on the back are much bigger than those in the tongue (data not shown). To our knowledge, the present study is the first *in vivo* fluorescent animal model for ACCM, which could prove to be invaluable for research of tumor invasion, angiogenesis, metastasis, and for the development of new therapies for this disease. In this tumor model, ACCM-GFP cells displayed the same characteristics as ACCM cells in cell proliferation, invasion ability, and Id-1 protein expression. This shows that the insertion of retroviral genome into ACCM had no influence on the physiologic behavior in our study.

siRNA is the most essential and well known dsRNA and it can be used as an effective therapeutic agent in those diseases caused due to elevated expression of genes. Such diseases include certain viral diseases, cancer, inflammatory diseases, HIV, influenza, polio, etc. [29]. For therapeutic purposes, it is essential to introduce dsRNA inside the cells, so that they can recognize the target genes and cause their suppression. In the present study, Id-1 gene was knocked down by lentivirus-mediated RNAi efficiently. Furthermore, lentivirus was applied for RNAi, which is currently considered very safe and practically possible owing to careful basic virology research and intensive vector development. The result proved that it is feasible to infect a cell line with viral vector twice without altering the cell physiology at molecular or morphologic levels.

As increasing evidence indicates that Id-1 plays a vital role on development and progression of oral cancer [30], the primary aim of this study was to determine whether RNAi-mediated suppression of Id-1 could be used to arrest the proliferative and motile characteristics of ACCM tumors and be demonstrated as a strategy for the gene therapy. First of all, Id-1 mRNA expression and protein level were significantly down-regulated in ACCM-GFP tumors infected with Id-1-siRNA-lentivirus indicating that RNAi successfully inhibited expression of the Id-1 gene. Additionally, the effect of gene silencing could maintain for at least 2 wk in our *in vivo* study. Our result of significant reduction is consistent with the close positive relationship between Id-1 and tumor development [31, 32]. However, it should be noted that the protein expression fell to a stable level 2 d later than mRNA expression. On the one hand, transcription under the direction of DNA occurs earlier than translation process by decoding mRNA. On the other hand, introduction of siRNA into cells raises concern as to whether the presence of "foreign" RNA may trigger pathogen pattern-recognition receptors that will alter normal cell properties [33]. A current model suggests that TLR-induced immunostimulation by RNA is determined by the length, sequence, form of RNA delivered, and the cell type studied [34]. In our opinion, multiple interactions might lead to the late change on protein level.

A 10 and 8 d plateau was shown for mRNA and protein reduction, respectively. In theory, non-RNAi tumor cells should multiply faster than those infected by lentivirus particles, which means less and less significant difference between the RNAi mice and controls on mRNA and protein level in the long run. Nevertheless, it seemed that mRNA and protein expression were reduced to a stable level for about 1 wk in our research. With the exception of dissection site and individual difference, cell proliferation ability should be taken into account. The stability of mRNA and protein expression after RNAi could be elucidated by the evidence that Id-1 was independent of cellular proliferation, and there was no relationship between Id-1 and Ki-67 [30]. Although this study [30] suggested that it is unlikely that Id-1 expression in oral carcinomas seems to reflect cell proliferation, the reduction of Ki-67 expression was indeed seen in our investigation. It proved that Ki-67 is still a widely used immuno-histochemical marker of cell proliferation [22, 35], and for salivary gland carcinomas, RNAi can cut down Ki-67 expression, which will result in inhibition of tumor growth. This result is in agreement with the study of Cheuk and Chan [36]. Therefore, further investigation is required for the mechanism involved.

In our experiment, significant decrease of Id-1 mRNA and protein expression appeared on the fourth day after RNAi; however it is on the 14th day that slowing down of tumor growth could be observed, indicating that clinical alteration could be detected around 2 wk after RNAi. We consider that this span should not be constant in that it depends on the transduction efficiency, which can be influenced by the tumor's pathologic type, viral viability, and effectiveness of injection. The average lifespan of the mice was around 2 wk after RNAi in our research, much shorter than with mice that had dorsal or lateral injections, resulting from systemic dyscrasia caused by eating disorder and respiratory failure. In fact, the short lifespan limited further study of the observation for tumor size alterations and tumor metastasis. However, we presumed that the tissue invaded by metastatic tumor cells that were treated with RNAi would appear with less fluorescence indicating fewer tumor cells metastasized than controls if the lifespan was much longer.

There are indications that Id-1 can not only antagonize the bHLH-mediated activation of well-known inhibitors of cell cycle progression, but also enhance the apoptosis [37]. Our results provided further evidence that Id-1 protein is associated with apoptotic pathways, which was consistent with the previous report [30]. Induction of tumor cell apoptosis in response to a large number of stimuli has proved to be an intriguing and promising antitumor approach [38]. In this regard, Id-1 should be considered as a potential target for ACCM treatment. Another characteristic feature of a malignant tumor is its ability to invade into surrounding and distal tissues. Our results further raised the possibility of Id-1 expression as a biological indicator to regulate ACCM cell invasion and a novel target in anti-neoplaston drug design.

The role of Id-1 protein in ACC remains unclear, although high expression of Id-1 protein was detected in ACC [13, 14]. A number of signaling pathways are known to mediate the tumorigenic effects of Id-1. For example, p16/Rb tumor suppressor [39, 40],

mitogen-activated protein kinase (MAPK) [41], and nuclear factor-kappaB (NF-κB) [42] are involved. Furthermore, Id-1 stimulates autocrine secretion of vascular endothelial growth factor (VEGF) [43, 44] to promote tumor angiogenesis. Based on the participation of phosphatidylinositol-3-kinase/protein kinase B (PI3 K/Akt) signaling pathway in ACC tumorigenesis [45] and the evidence that Id-1 is an upstream regulator of the PI3 K/Akt pathway [46], we infer that down-regulation of mouse double minute 2 (MDM2) [47], a direct target of Akt, resulted from RNAi of Id-1 can lead to inhibition of cell proliferation by directly inactivating E2F-1[48], which will effect driving G1/S progression of ACC cells. Additionally, Id-1 knockdown can decrease the resistance to tumor necrosis factor-alpha (TNF-α)-induced apoptosis [46, 49]. The deregulation of the Bcl-2 family genes, Bax, Bcl-2, or Bcl-xl mediates the Id-1 antiapoptotic effect. Since PI3 K/Akt/NF-κB is documented to be involved in the regulation of cellular invasion and metastasis [47, 50], it may be one of the mechanisms by which Id-1 exerts its effects on cancer progression.

Although RNAi effectively exerted an anticarcinomic effect on ACCM, issues related to transfecting cells should be considered. Viruses can be administered by an intratumoral injection of the viral supernatant, the intratumoral implantation of a polymeric device that can release viral vectors locally, or by an i.v. injection of the viral supernatant through the tail vein. The xeno-implantation may result in interference with the development of the tumor. The bio-distribution and rate of accumulation of virus following an i.v. injection will depend on the virus type, total surface area of the microvessel, microvascular permeability, and rate of cellular uptake [51]. In spite that previous study involving BALB/c mice showed i.v. injection of lentivirus through the tail vein led to stable GFP expression sustained for 40 d [52], we prefer multiple intratumoral injections for the reason that neither effect by implantation on tumor growth nor permeation will appear. As we know, the transduction efficiency *in vivo* is less than *in vitro*, and it is difficult to ascertain the transduction efficiency achieved by local injection. Therefore, the transduction efficiency was the most crucial factor in the whole experiment.

The field of RNAi is moving forward with a remarkable pace, and several clinical trials are being conducted to assess the safety and efficacy of this approach. However, apart from hazards of vector integration, stable endogenous siRNA expression could be potentially harmful because of activation of innate immunity, off-target effects as well as interference with the endogenous miRNA pathway. In addition, siRNA could be rendered ineffective by generation of escape mutants in viral infections. In a short span of time, great progress has been made in addressing some of these issues, such as the improvement in siRNA design, development of multiplex siRNAs, and inducible expression systems. Despite these commendable achievements, further improvements in safety, efficacy, and reliability will be required before the lentiviral RNAi-based therapies become clinically viable.

From a therapeutic standpoint, since Id-1 is overexpressed in ACCs [13, 14] but presents at very low levels in normal adult tissues [53], inhibition of Id-1 should have very little side effect on normal tissues. Furthermore, with the development of improved delivery systems in RNAi technology and the recent success in application of therapeutic siRNA in nonhuman primates [54], RNAi-based silencing of Id-1 may be a promising strategy, which will contribute to the therapy for ACCs.

ACKNOWLEDGMENTS

This project was partly sponsored by National Natural Science Foundation of China (30672339 to SHL and 0772269 to FCW), and SRF for ROCS, SEM to SHL.

REFERENCES

1. Fordice J, Kershaw C, El-Naggar A, et al. Adenoid cystic carcinoma of the head and neck. Predictors of morbidity and mortality. Arch Otolaryngol Head Neck Surg 1999;125:149.
2. Umeda M, Nishimastsu N, Masago H, et al. Tumor-doubling time and onset of pulmonary metastasis from adenoid cystic carcinoma of the salivary gland. Oral Surg Oral Med Oral Pathol 1999;88:473.
3. de Kerviler E, Bely N, Laccourreye O, et al. The aryepiglottic fold as a rare location of adenoid cystic carcinoma. Am J Neuroradio 1995;116:1375.
4. Dan H, Wangtao C, Ronggen H, et al. Different cDNA microarray patterns of gene expression reflecting changes during metastatic progression in adenoid cystic carcinoma. World J Sur Onc 2003;1:28.
5. Klosek SK, Nakashiro K, Hara S, et al. CD151 forms a functional complex with c-Met in human salivary gland cancer cells. Biochem Biophys Res Commun 2005;336:408.
6. Perk J, Iavarone A, Benezra R. Id family of helix-loop-helix proteins in cancer. Nat Rev Cancer 2005;5:603.
7. Duxbury MS, Matros E, Ito H, et al. Systemic siRNA-mediated gene silencing: A new approach to targeted therapy of cancer. Ann Surg 2004;240:667.
8. Han S, Gou C, Hong L, et al. Expression and significances of Id1 helix-loop-helix protein overexpression in gastric cancer. Cancer Lett 2004;216:63.
9. Schoppmann SF, Schindl M, Bayer G, et al. Overexpression of Id-1 is associated with poor clinical outcome in node negative breast cancer. Int J Cancer 2003;104:677.
10. Ouyang XS, Wang X, Lee DT, et al. Overexpression of ID-1 in prostate cancer. J Urol 2002;167:2598.
11. Schindl M, Schoppmann SF, Ströbel T, et al. Level of Id-1 protein expression correlates with poor differentiation, enhanced malignant potential, and more aggressive clinical behavior of epithelial ovarian tumors. Clin Cancer Res 2003;9:779.
12. Tsuchiya T, Okaji Y, Tsuno NH, et al. Targeting Id1 and Id3 inhibits peritoneal metastasis of gastric cancer. Cancer Sci 2005;96:784.

13. Pei L, Shaohua L, Hongshun Q, et al. Effects of silencing Id-1 in cell culture of human adenoid cystic carcinoma. Oral Oncol 2009; 45:783.
14. Xie W, Li X, Guoxin R, et al. Expression and importance of inhibitor of DNA binding helix-loop-helix protein in salivary adenoid cystic carcinoma. Br J Oral Maxillofac Surg 2009;9 10.1016/j.bjoms.2009.08.008.
15. Schindl M, Oberhuber G, Obermair A, et al. Overexpression of Id-1 protein is a marker for unfavorable prognosis in early-stage cervical cancer. Cancer Res 2001;61:5703.
16. Li J, Jia H, Xie L, et al. Correlation of inhibitor of differentiation 1 expression to tumor progression, poor differentiation and aggressive behaviors in cervical carcinoma. Gynecol Oncol 2009; 114:89.
17. Coppe JP, Smith AP, Desprez PY. Id proteins in epithelial cells. Exp. Cell Res 2003;285:131.
18. Sikder HA, Devlin MK, Dunlap S, et al. Id proteins in cell growth and tumorigenesis. Cancer Cell 2003;3:525.
19. Fire A, Xu S, Montgomery MK, et al. Potent and specific genetic interference by double- stranded RNA in *Caenorhabditis elegans*. Nature 1998;391:806.
20. Hshitani S, Urade M, Zushi Y, et al. Establishment of nude mouse transplantable model of a human adenoid cystic carcinoma of the oral floor showing metastasis to the lymph node and lung. Oncol Rep 2007;17:67.
21. Li J, Piao YF, Jiang Z, et al. Silencing of signal transducer and activator of transcription 3 expression by RNA interference suppresses growth of human hepatocellular carcinoma in tumor-bearing nude mice. World J Gastroenterol 2009;21:2602.
22. Singh A, Boldin-Adamsky S, Thimmulappa RK, et al. RNAi-mediated silencing of nuclear factor erythroid-2-related factor 2 gene expression in non-small cell lung cancer inhibits tumor growth and increases efficacy of chemotherapy. Cancer Res 2008;68:7975.
23. Wang QZ, Xu W, Habib N, et al. Potential uses of microRNA in lung cancer diagnosis, prognosis, and therapy. Curr Cancer Drug Targets 2009;9:572.
24. Selkirk SM. Gene therapy in clinical medicine. Postgrad Med J 2004;80:560.
25. Duan XJ, Yang L, Zhou Y, et al. Influence of fluorescent protein expression on the proliferation of NIH3T3 cells in vitro. Zhonghua Shao Shang Za Zhi 2005;21:374.
26. Duan XJ, Yang L, Zhou Y, et al. Application of enhanced green fluorescent protein labeling technology to monitoring marrow mesenchymal stem cells migration after bone fracture. Zhongguo Xiu Fu Chong Jian Wai Ke Za Zhi 2006;20:102.
27. Livak KJ, Schmittgen TD. Analysis of relative gene expression data using real-time quantitative PCR and the 2 (-Delta Delta C(T)) Method. Methods 2001;25:402.
28. Arap W, Pasqualini R, Ruoslahti E. Cancer treatment by targeted drug delivery to tumor vasculature in a mouse model. Science 1998;279:377.
29. Kumar A. RNA interference: A multifaceted innate antiviral defense. Retrovirology 2008;5:17.
30. Nishimine M, Nakamura M, Mishima K, et al. Id proteins are overexpressed in human oral squamous cell carcinomas. J Oral Pathol Med 2003;32:350.
31. Darby S, Cross SS, Brown NJ, et al. BMP-6 over-expression in prostate cancer is associated with increased Id-1 protein and a more invasive phenotype. J Pathol 2008;214:394.
32. McAllister SD, Christian RT, Horowitz MP, et al. Cannabidiol as a novel inhibitor of Id-1 gene expression in aggressive breast cancer cells. Mol Cancer Ther 2007;6:2921.
33. Zhang L, Procuik M, Fang T, et al. Functional analysis of the quantitative expression of a costimulatory molecule on dendritic cells using lentiviral vector-mediated RNA interference. J Immno Methods 2009;344:87.
34. Robbins MA, Rossi JJ. Sensing the danger in RNA. Nat Med 2005;11:250.
35. Zheng J-N, Pei D-S, Mao L-J, et al. Inhibition of renal cancer cell growth in vitro and *in vivo* with oncolytic adenovirus armed short hairpin RNA targeting Ki-67 encoding mRNA. Cancer Gene Ther 2009;16:20.
36. Cheuk W, Chan JK. Advances in salivary gland pathology. Histopathology 2007;51:1.
37. Prabhu S, Ignatova A, Park ST, et al. Regulation of the expression of cyclin-dependent kinase inhibitor p21 by E2A and Id proteins. Mol Cell Biol 1996;17:5888.
38. Sellers WR, Fisher DE. Apoptosis and cancer drug targeting. J Clin Invest 1999;104:1655.
39. Ouyang XS, Wang X, Ling MT, et al. Id-1 stimulates serum independent prostate cancer cell proliferation through inactivation of p16(INK4a)/pRB pathway. Carcinogenesis 2002;23:721.
40. Lee TK, Man K, Ling MT, et al. Over-expression of Id-1 induces cell proliferation in hepatocellular carcinoma through inactivation of p16(INK4a)/pRB pathway. Carcinogenesis 2003;24:1729.
41. Ling MT, Wang X, Ouyang XS, et al. Activation of MAPK signaling pathway is essential for Id-1 induced serum independent prostate cancer cell growth. Oncogene 2002;21:8498.
42. Ling MT, Wang X, Ouyang XS, et al. Id-1 expression promotes cell survival through activation of NF-κB signaling pathway in prostate cancer cells. Oncogene 2003;22:4498.
43. Lyden D, Young AZ, Zagzag D, et al. Id1 and Id3 are required for neurogenesis, angiogenesis and vascularization of tumor xenografts. Nature 1999;401:670.
44. Ling MT, Lau TC, Zhou C, et al. Overexpression of Id-1 in prostate cancer cells promotes angiogenesis through the activation of vascular endothelial growth factor (VEGF). Carcinogenesis 2005;26:1668.
45. Maruya SI, Myers JN, Weber RS, et al. ICAM-5(telencephalin) gene expression in head and neck squamous carcinoma tumorigenesis and perineural invasion. Oral Oncol 2005;41:580.
46. Li B, Cheung PY, Wang X, et al. Id-1 activation of P13K/Akt/NFkapaB signaling pathway and its significance in promoting survival of esophageal cancer cells. Carcinogenesis 2007; 28:2313.
47. Bader AG, Kang S, Zhao L, et al. Oncogenic P13K deregulates transcription and translation. Nat Rev Cancer 2005;5:921.
48. Martin K, Trouche D, Haqemeier C, et al. Stimulation of E2F1/DP1 transcriptional activity by MDM2 oncoprotein. Nature 1995;375:691.
49. Zhang X, Ling MT, Wang X, et al. Inactivation of Id-1 in prostate cancer cells: A potential therapeutic target i inducing chemosensitization to Taxol through activation of JNK pathway. Int J Cancer 2006;118:2072.
50. Karin M, Cao Y, Greten FR, et al. NF-κB in cancer: From innocent bystander to major culprit. Nat Rev Cancer 2002;2:301.
51. Wang Y, Yuan F. Delivery of viral vectors to tumor cells: Extracellular transport, systemic distribution, and strategies for improvement. Ann Biomed Eng 2006;34:114.
52. Pan D, Gunther R, Duan W, et al. Biodistribution and toxicity studies of VSVG-pseudotyped lentiviral vector after intravenous administration in mice with the observation of *in vivo* transduction of bone marrow. Mol Ther 2002;6:19.
53. Wong YC, Wang X, Ling MT. Id-1 expression and cell survival. Apoptosis 2004;9:279.
54. Zimmermann TS, Lee AC, Akinc A, et al. RNAi-mediated gene silencing in non-human primates. Nature 2006;441:111.